Polymer Bulletin 54, 75–84 (2005)
DOI 10.1007/s00289-005-0365-6

Polymer Bulletin

Rheology, Morphology and Estimation of Interfacial Tension of LDPE/EVA and HDPE/EVA Blends

H.A. Khonakdar (✉)[1], S.H. Jafari [2,3], A. Yavari [2], A. Asadinezhad [2], U. Wagenknecht [3]

1) Department of Polymer Processing, Iran Polymer and Petrochemical Institute (IPPI),
P.O.Box: 14965-115, Tehran, Iran
2) Department of Chemical Engineering, Faculty of Engineering, University of Tehran,
P.O.Box: 11365/4563, Tehran, Iran
3) Leibniz Institute of Polymer Research Dresden, Hohe Str. 6, D-01069 Dresden, Germany
E-mail: H.khonakdar@ippi.ac.ir, halikh@yahoo.com, Fax: +98-21-4580021

Received: 29 December 2004 / Revised version: 23 February 2005 / Accepted: 3 March 2005

Summary

Rheological characteristics and morphology of low-density polyethylene (LDPE) /ethylene vinyl acetate copolymer (EVA) and high-density polyethylene (HDPE)/EVA blends were compared. Morphological examinations clearly reveal a two-phase morphology in which the LDPE/EVA blends have smaller dispersed domain size than HDPE/EVA Furthermore, LDPE/EVA shows a finely interconnected morphology at 50wt% of EVA while HDPE/EVA exhibits a coarse co-continuous morphology at the same composition. The morphological observations can be attributed to the lower viscosity ratio and lower interfacial tension in the LDPE/EVA system. The Palierne model also successfully fits to the experimental data giving higher values for interfacial tension of HDPE/EVA system as compared to LDPE/EVA.

Introduction

Blending two or more polymers is an effective strategy to improve plastic material performance. The procedure is to use common polymers and to blend them in the melt to accomplish the required properties. However, most polymer pairs are immiscible and form a multiphase system leading to a more complex rheology. Furthermore, the end-use performance of the blend is influenced by final morphology which itself is substantially affected by rheological behavior of the system [1-4].

Most of the studies devoted to date consider the rheological behavior of immiscible blends [5-10]. In these systems, interfacial tension has a controlling role on both rheology and morphology since it influences the dispersed particle size as well as particle size distribution. The interfacial tension is governed by the structural similarity of the components, blend composition, and addition of a compatibilizer [11].

A most useful analysis for emulsions with viscoelastic matrix and dispersed phase is the Palierne model [12] widely been employed to explain the rheology of several blend systems [5,13-18]. Interfacial tension can be estimated using particle size values via this model as already shown by Asthana et al. [13] and Shi et al. [14]. However, several efforts have been made to investigate the rheology and morphology of polyethylene and EVA blends [5,19-23], but to the best of our knowledge, no attempt has been focused on the rheological behavior of LDPE/EVA and HDPE/EVA systems and estimation of their interfacial tension values from a comparative viewpoint.

In our previous work [24] we compared the dynamic mechanical behavior and morphology of LDPE/EVA and HDPE/EVA blends. In this work we aim to compare the rheology and morphology of these systems in different blend ratios. We will also analyze the experimental data by means of the Palierne model to estimate the interfacial tension.

Experimental

Materials

HDPE grade MG7547A, with MFI of 4.0 g/10 min. and density of 954 kg/m^3 was supplied by Borealis, Denmark. LDPE grade LD 00BW, with MFI of 2.0 g/10 min and density of 923 kg/m^3 was obtained from Exxon Mobile Co., Germany. EVA copolymer grade UL 00218, containing 18% VA, with MFI of 1.7 g/10 min and density of 938 kg/m^3 was obtained from Exxon Mobile Co., Germany. Irganox 1010 antioxidant with density of 1.15 g/cm^3 was purchased from Ciba Co., Switzerland.

Instruments

LDPE/EVA and HDPE/EVA blends in different amounts of EVA (0 to 100 wt%) were melt mixed in an internal mixer (Plasti- Corder, PL 2000, BRABENDER) at 50 rpm and 145°C for 10 min, subsequently compression molded to flat sheets using

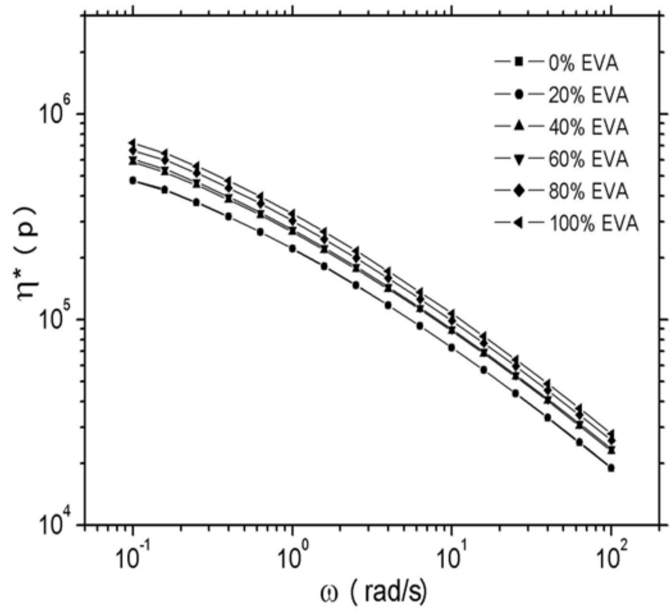

Figure 1. Complex viscosity of LDPE/EVA blends at 150°C.

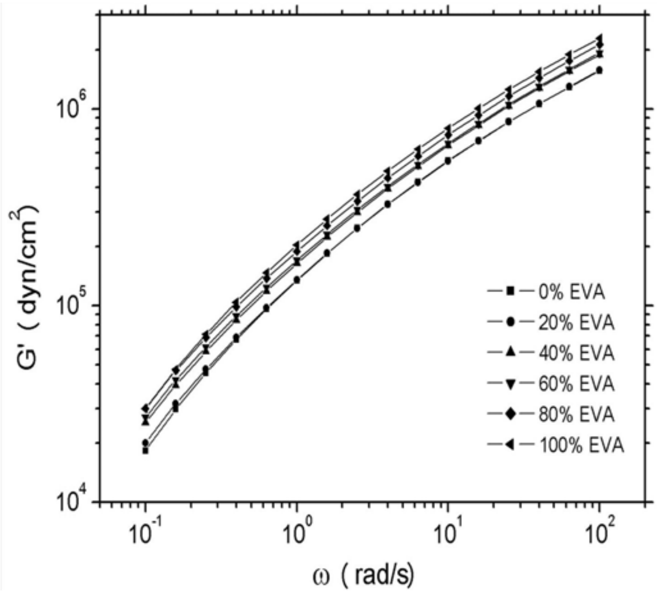

Figure 2. Storage modulus of LDPE/EVA blends at 150°C.

Fontune 400 KN laboratory hot press at 190°C for 3 min under 10 MPa pressure, then cooled at rate of 15 K/min to ambient temperature. Dynamic rheological examinations were carried out using a parallel plate ARES Rheometer (Rheometric Inc.,) on properly dried samples under dry nitrogen atmosphere in a frequency range of 10^{-1}-10^{2} rad/s. Disk shaped samples with 25 mm diameter and 1.5 mm thickness were pressed using a Carver laboratory press. Strain sweep tests were performed first to determine the linear viscoelastic zone at very low strains (0.5-5%). Scanning electron microscopy (SEM) was employed to study the morphology of the blends. Cryofractured surfaces of the samples were chemically etched by 1,2- dichloroethane solvent for 1.5 h at 70°C in order to remove the EVA component, subsequently gold sputtered after proper drying and observed under a LEO 435 VP (LEO Electronenmikroskopie, Germany) SEM.

Results and Discussion

Rheology

LDPE/EVA System. The storage shear modulus and complex viscosity as a function of angular frequency at different blend ratios for LDPE/EVA blends are illustrated in Figures 1 and 2, respectively. Both rheological parameters increase upon addition of EVA content. Zero-shear viscosity values in logarithmic scale for LDPE/EVA system in different blend ratios derived using Carreau model [25] are displayed versus EVA content in Figure 3 following a linear trend which implies that the rheological parameters of the blend obey a logarithmic mixing rule. However, no discernible change is observed upon addition of 20wt% EVA which may be due to phase separation of the system at this composition. To further analyze the rheological data, we used the Cole-Cole technique developed by Han et al. [26] in which log G' is plotted versus log G'' and is a useful tool to assess the blend morphological state.

Figure 4 demonstrates the Cole-Cole plot for LDPE/EVA blends. One can see that the respective *G′*-*G″* curves for LDPE/EVA blends are all linear and show a composition-independent correlation indicating a similar morphological state and high degree of compatibility in the system [21,22]. This essentially originates from the existence of the structural similarity (microstructure) between blend constituents.

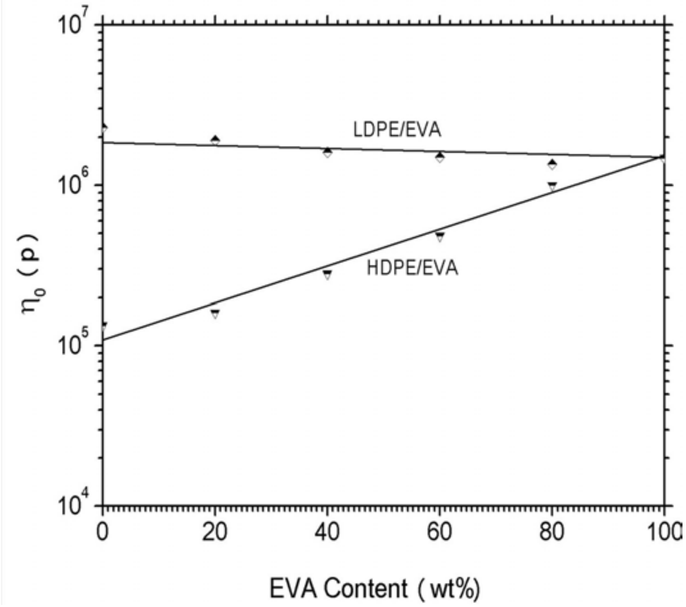

Figure 3. Zero-shear viscosity change of both systems against EVA content at 150°C.

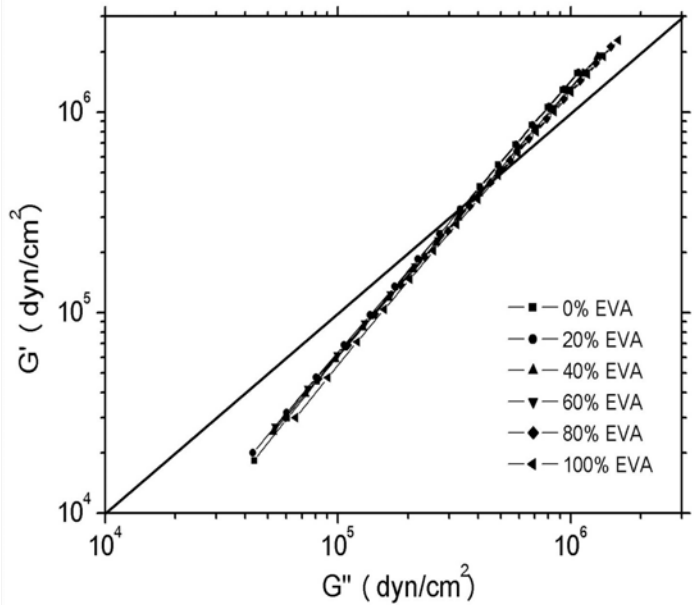

Figure 4. Cole-Cole diagram of LDPE/EVA system.

HDPE/EVA System. The dynamic rheological parameters of HDPE/EVA blends with various compositions as a function of angular frequency given in Figures 5 and 6 also obey the logarithmic rule of mixtures with regards to Figure 3. It can be observed from Cole-Cole diagram for this system (Figure 7) that the morphological state of HDPE/EVA blends, based upon Han analysis [26], is similar. However a composition-dependent correlation appears suggesting a lower degree of compatibility in this system compared to LDPE/EVA.

Morphology

Figures 8 and 9 show the SEM micrographs of the LDPE/EVA and HDPE/EVA blends containing various amounts of EVA. It can be observed that both blends exhibit a two-phase morphology implying the immiscibility of the blends which has also reported by Takidis et al.[22]. Moreover, The size of dispersed domains at low EVA content (up to 20 wt%) falls within the range of submicron to about 2μm, whereas at higher EVA content particularly for HDPE/EVA blends, the EVA domains size significantly increases and at higher EVA content (around 50/50 wt/wt) it approaches the phase inversion region. A comparison of the LDPE/EVA and HDPE/EVA blends reveals that the former blend has smaller dispersed droplet size which is attributed to the higher viscosity ratio in the latter system. The LDPE/EVA system also exhibits a co-continuous morphology at 50% EVA content, in which both phases are finely interconnected, while the HDPE/EVA system shows a coarse morphology at this blend composition that is also ascribed to higher viscosity ratio in the latter system.

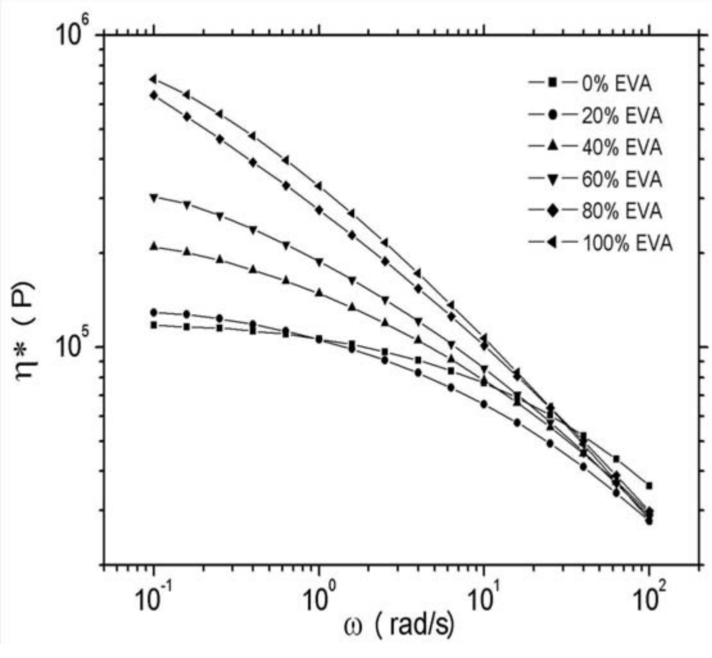

Figure 5. Storage shear modulus of HDPE/EVA blends at 150°C.

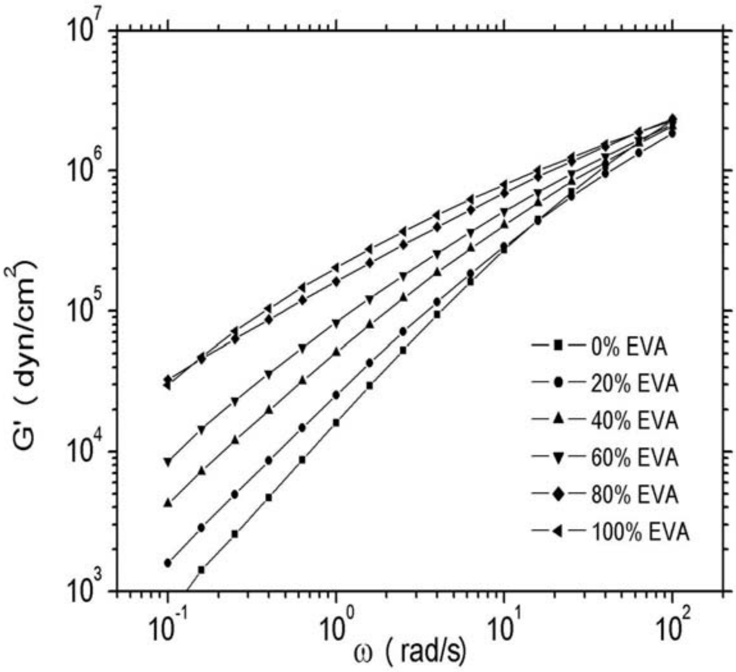

Figure 6. Complex viscosity of HDPE/EVA blends at 150°C.

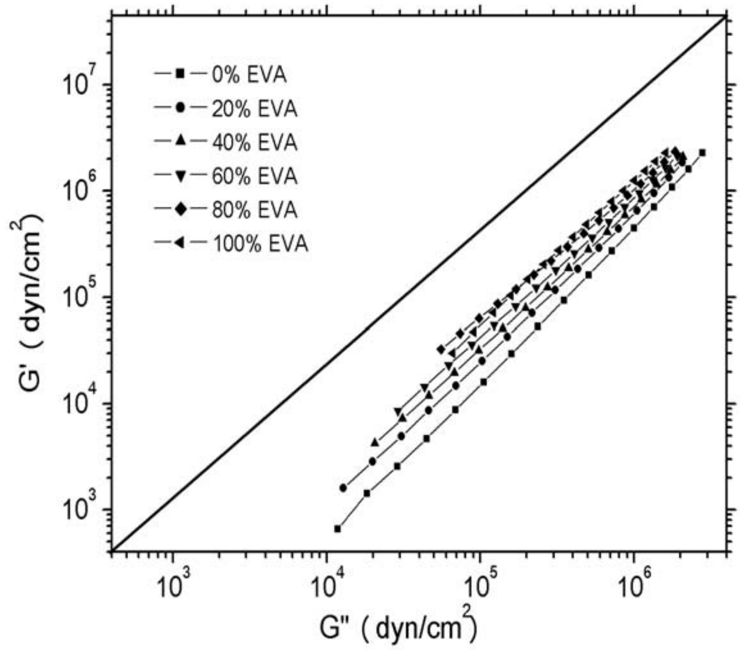

Figure 7. Cole-Cole diagram of HDPE/EVA blends at 150°C.

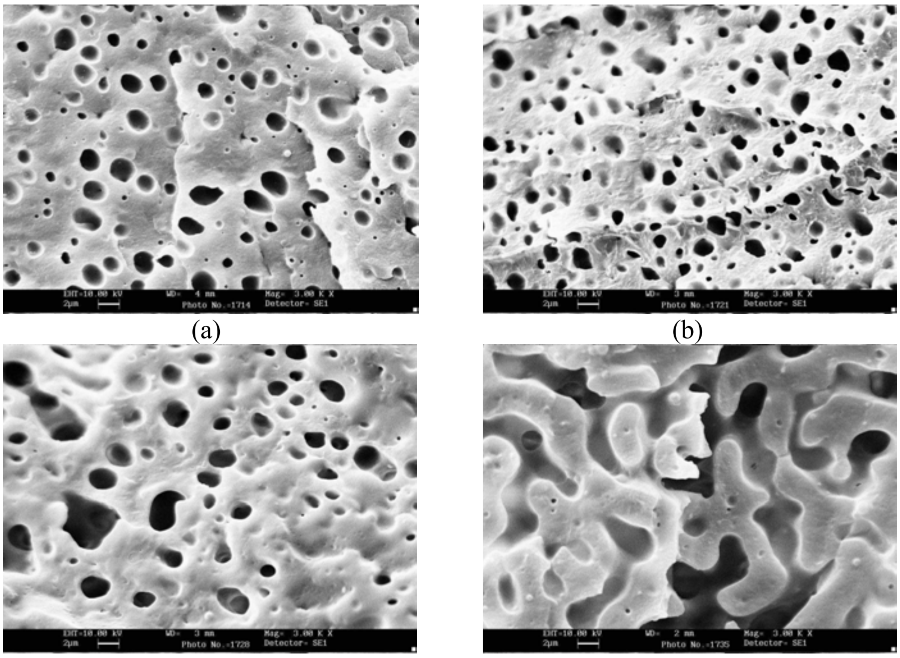

(a) (b) (c) (d)

Figure 8. SEM micrographs of LDPE/EVA: (a) 20; (b) 30; (c) 40; (d) 50 wt% EVA.

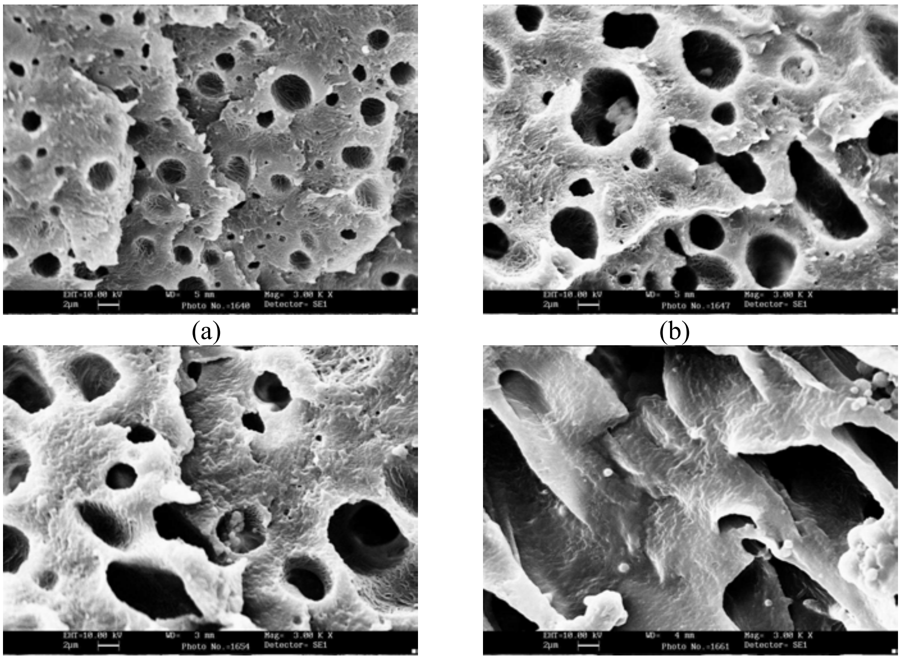

(a) (b) (c) (d)

Figure 9. SEM micrographs of HDPE/EVA blends: (a) 20; (b); 30 (c); 40 (d); 50 wt% EVA.

Palierne Analysis

A simplified form of the Palierne model [12] developed by Graebling et al. [27] assuming monodisperse particle size distribution is written as,

$$G_b^* = G_m^* \frac{1+3\varphi.H(\omega)}{1-2\varphi.H(\omega)} \tag{1}$$

where

$$H(\omega) = \frac{(4\alpha/R_d)(2G_m^*(\omega)+5G_d^*(\omega)) + (G_d^*(\omega)-G_m^*(\omega))(16G_m^*(\omega)+19G_d^*(\omega))}{(40\alpha/R_d)(G_m^*(\omega)+G_d^*(\omega)) + (2G_d^*(\omega)+3G_m^*(\omega))(16G_m^*(\omega)+19G_d^*(\omega))}$$

in which, R_d and φ denote the radius and the volume fraction of dispersed phase, respectively, while $G^*_b(\omega)$, $G^*_m(\omega)$, $G^*_d(\omega)$, α , and ω represent complex modulus of blend, matrix and dispersed phase, interfacial tension, and strain frequency, respectively.

The number average particle size values obtained from morphological examinations and used in the model, are given in Table 1. Figures 10 and 11 illustrate a comparison of the experimental data and theoretical predictions by the Palierne model. It is evident that this model satisfactorily fits to the experimental data by a fitting parameter of ca. α = 1 dyn/cm for LDPE/EVA and ca. α = 2 dyn/cm for HDPE/EVA system, although it shows some deviations at high dispersed-phase contents especially near the intermediate compositions which has already been reported for blends of metallocene polyethylene and EVA by Peon et al. [5]. A comparison on the derived values for interfacial tension of both systems demonstrates a more structural similarity between LDPE and EVA chains compared to HDPE and EVA previously suggested by both rheological and morphological results.

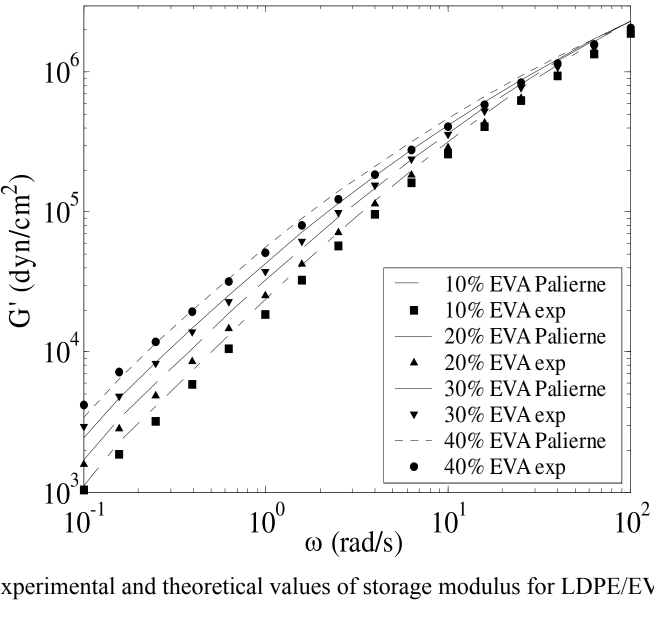

Figure 10. Experimental and theoretical values of storage modulus for LDPE/EVA blends.

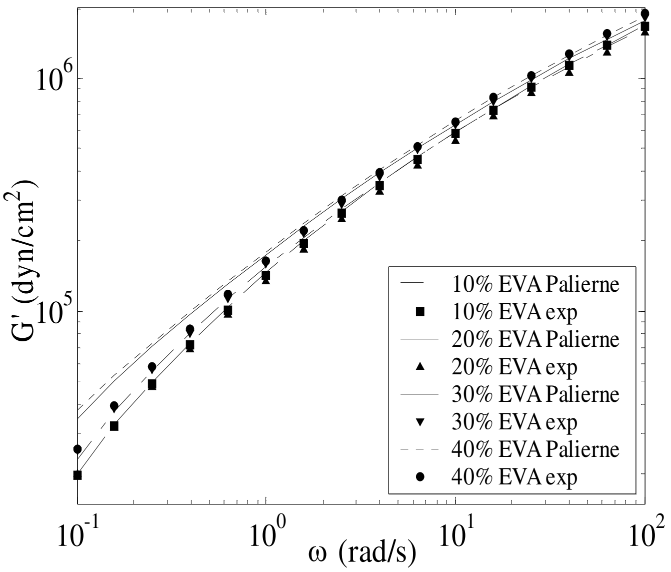

Figure 11. Experimental and theoretical values of storage modulus for HDPE/EVA blends.

Table 1. The values of number average particle radius used in the Palierne analysis.

Sample	R_d (μm)
LDPE/EVA 90/10	0.38
LDPE/EVA 80/20	0.91
LDPE/EVA 70/30	1.00
LDPE/EVA 60/40	1.16
HDPE/EVA 90/10	0.49
HDPE/EVA 80/20	0.97
HDPE/EVA 70/30	1.97
HDPE/EVA 60/40	2.82

Conclusions

A comparison on the morphology and rheological characteristics of LDPE/EVA and HDPE/EVA systems was carried out. Rheological examinations showed that the complex viscosity and shear modulus of both blends fell between those of neat components following a logarithmic mixing rule. Morphological examinations clearly revealed a phase-separated morphology for both systems in which the droplet size of LDPE/EVA system is smaller than that of HDPE/EVA attributed to lower interfacial tension as well as lower viscosity ratio in the former blend. Furthermore, at 50% EVA content, the former system exhibited a co-continuous morphology, in which both phases are finely interconnected, while the latter system showed a coarse morphology also ascribed to higher viscosity ratio and higher interfacial tension in the latter system because of less similar macromolecular structures. A good fit of the Palierne model to the experimental data was also observed giving higher values for interfacial tension of HDPE/EVA system as compared to LDPE/EVA.

Acknowledgements. The authors thank Dr. Mirzadeh, Dr. Esfandeh, Dr. Leuteritz, and Mrs. Jentzsch for their technical assistance.

References

1. Supaphol P, Dangseeyun N, Thanomkiat P, Nithitanakul M (2004) J Polym Sci Polym Phys 42:676
2. Aravind I, Albert P, Ranganathaiah C, Kurian JV, Thomas S (2004) Polymer 45:4925
3. Dharaiya D, Jana SC, Shafi A (2003) Polym Eng Sci 43:580
4. Kong Y, Hay JN (2002) Polymer 43:1805
5. Peon J, Vega JF, Amo BD, Martınez-Salazar J (2003) Polymer 44:2911
6. Zhang ZL, Zhang HD, Yang YL, Vinckier I, Laun HM (2001) Macromolecules 34: 1416
7. Jeon HS, Nakatani AI, Han CC, Colby RH (2000) Macromolecules 33: 973
8. Castro M, Carrot C, Prochazka F (2004) Polymer 45 : 4095
9. Kernick WA, Wagner N J (1999) J Rheol 43:521
10. Xu SA, Zhu L, Xie JW, Jiang M (1999) Polym Int 48 :1113
11. Moan M, Huitric P, Médéric P, Jarrin J (2000) J Rheol 44:1227
12. Palierne JF (1990) Rheol Acta 29:204
13. Asthana H, Jayaraman K (1999) Macromolecules 32: 3412
14. Shi D, Ke Z, Yang J, Gao Y,Wu J,Yin J (2002) Macromolecules 35:8005
15. Bousmina M (1999) Rheol Acta 38:73
16. Hemelrijck EV, Puyvelde PV, Velankar S, Macosko CW Moldenaers P (2004) J Rheol 48:143
17. Minale M, Moldenaers P, Mewis J (1997) Macromolecules 30:5470
18. Vinckier I, Laun HM (1999) Rheol Acta 38:274
19. Peon J, Aguilar M, Vega JF, Amo BD, Martınez-Salazar J (2003) Polymer 44:1589
20. Peon J, Vega JF, Aroca M, Martınez-Salazar J (2001) Polymer 42:8093
21. Wu T, Li Y, Zhang DL, Liao SQ, Tan HM (2004) J Appl Polym Sci 91: 905
22. Takidis G, BikiarisDN, Papageorgiou GZ, Achilias DS, Sideridou I (2003) J Appl Polym Sci 90:841
23. Moly KA, Bhagawan SS, Thomas S (2002) Mat Letters 53:346
24. Khonakdar HA, Wagenknecht U, Jafari SH, Hassler R, Eslami H (2004) Adv Polym Tech 23:307
25. Carreau PJ (1968) PhD Thesis, Department of Chemical Engineering, University of Wisconsin
26. Han CD, Lem KW (1983) Polym Eng Rev 12:135
27. Graebling D, Froelich D, Muller R (1989) J Rheol 33:1283